Environmental and Molecular Mutagenesis 45:365–373 (2005)

In Vivo Mutagenesis Induced by Benzo[*a*]pyrene Instilled Into the Lung of *gpt* delta Transgenic Mice

Akiko H. Hashimoto,[1] Kimiko Amanuma,[1] Kyoko Hiyoshi,[1,2] Hirohisa Takano,[1] Ken-ichi Masumura,[3] Takehiko Nohmi,[3] and Yasunobu Aoki[1]*

[1]*Research Center for Environmental Risk, National Institute for Environmental Studies, Ibaraki, Japan*
[2]*Graduate School of Comprehensive Human Sciences, University of Tsukuba, Ibaraki, Japan*
[3]*Division of Genetics and Mutagenesis, National Institute of Health Sciences, Tokyo, Japan*

Benzo[*a*]pyrene (B[*a*]P) is a ubiquitous airborne pollutant whose mutagenicity has been evaluated previously by oral and intraperitoneal administration to experimental animals. In this study, mutagenesis in the lungs, the target organ of air pollutants, was examined after a single intratracheal instillation of 0–2 mg B[*a*]P into *gpt* delta transgenic mice. Intratracheal injection of B[*a*]P resulted in a statistically significant and dose-dependent increase in *gpt* mutant frequency as measured by 6-thioguanine selection. The mutant frequencies at B[*a*]P doses of 0.5, 1, and 2 mg were 2.8, 4.2, and 6.8 times higher than the frequency seen in nontreated mice ($0.60 \pm 0.13 \times 10^{-5}$). The most frequent mutations induced by B[*a*]P treatment were G:C→T:A transversions, which are characteristic of B[*a*]P mutagenesis in other models, and single-base deletions of G:C base pairs. To characterize the hotspots of B[*a*]P-induced mutations in the *gpt* gene, we analyzed sequences adjacent to the mutated G:C base pairs. Guanine bases centered in the nucleotide sequences CGT, CGA, and CGG were the most frequent targets of B[*a*]P. Our results indicate that intratracheal instillation of B[*a*]P into *gpt* delta mice causes a dose-dependent increase in *gpt* mutant frequency in the lung, and that the predominant mutation induced is G:C→T:A transversion. Environ. Mol. Mutagen. 45:365–373, 2005.

Key words: benzo[*a*]pyrene; *gpt* delta transgenic mouse; 6-thioguanine selection

INTRODUCTION

Benzo[*a*]pyrene (B[*a*]P), one of the most potent mutagens in ambient air, is generated by the combustion of fossil fuels such as occurs in diesel engines and industrial settings. This polycyclic aromatic hydrocarbon (PAH), also a component of cigarette smoke and burned foods, is carcinogenic in rodent cancer bioassays [Singh et al., 1998; Iwagawa et al., 1989]. B[*a*]P is converted to reactive intermediates, B[*a*]P diol epoxides. Of these intermediates, benzo[*a*]pyrene 7,8-diol-9,10-epoxide (BPDE) is the most mutagenic [Miller et al., 2000], but all of the B[*a*]P diol epoxide enantiomers are carcinogenic in mammals [Buening et al., 1978]. The metabolism of B[*a*]P is catalyzed in various tissues by mono-oxygenases of the cytochrome P-450 (CYP) 1A family. Expression of the genes encoding these mono-oxygenases is mediated by the arylhydrocarbon receptor, a ligand-dependent transcription factor to which B[*a*]P and related PAHs bind. BPDE and other reactive metabolites are known to form DNA adducts, predominantly by binding to the exocyclic amino groups of guanine and adenine [Cosman et al., 1992; Bartsch, 1996]. The metabolites produced in the lung are qualitatively similar to those found in the liver and other tissues [Cohen et al., 1976; Prough et al., 1979; International Programme on Chemical Safety, 1998].

DNA adducts can cause mispairing of DNA bases, leading to the induction of mutations through the DNA replication process. The mutagenicity of B[*a*]P has been evaluated in several rodent tissues, including the liver, forestomach, and bone marrow, by exposing the transgenic

Grant sponsor: The Japan Society for the Promotion of Sciences; Grant number: 14207100.

*Correspondence to: Yasunobu Aoki, National Institute for Environmental Studies, 16-2 Onogawa, Tsukuba, Ibaraki 305-8506, Japan. E-mail: ybaoki@nies.go.jp

Received 21 May 2004; provisionally accepted 26 June 2004; and in final form 10 October 2004

DOI 10.1002/em.20098

Published online 18 January 2005 in Wiley InterScience (www.interscience.wiley.com).

TABLE I. Raw Data for Mutants Induced in the Lungs of *gpt* delta Mice After B[*a*]P Treatment[a]

B[*a*]P (mg)	ID of animals	Number of colonies		Mutant frequency ($\times 10^{-5}$)	Average mutant frequency ± SD ($\times 10^{-5}$)	% independent mutations[b]	Mutation frequency ($\times 10^{-5}$)	Average mutation frequency ± SD ($\times 10^{-5}$)
		Mutant	Total					
Control	1	5	800,800	0.62		80	0.50	
	2	5	1,113,600	0.45		100	0.45	
	3	5	702,400	0.71	0.60 ± 0.13	100	0.71	0.55 ± 0.14
	Total	15	2,616,800					
0.5	1	9	501,600	1.79		71	1.28	
	2	3	209,600	1.43		100	1.43	
	3	5	272,000	1.84	1.69 ± 0.22	80	1.47	1.39 ± 0.10
	Total	17	983,200					
1	1	11	499,200	2.20		88	1.93	
	2	14	556,800	2.51		100	2.51	
	3	35	1,225,600	2.86	2.52 ± 0.33[c]	60	1.72	2.05 ± 0.42
	Total	60	2,281,600					
2	1	53	1,088,800	4.87		82	3.98	
	2	46	1,420,000	3.24	4.05[e] [f]	70	2.27	3.13[d] [f]
	Total	99	2,508,800					

[a]Statistical significance was determined using an ANOVA test and the Scheffe test. Significant differences between the control and B[*a*]P-treated groups as indicated.
[b]Calculated from data in Table III.
[c]$P < 0.05$.
[d]$P < 0.01$.
[e]$P < 0.001$.
[f]Average of two animals.

Muta Mouse and Big Blue mouse models to B[*a*]P either orally or by i.p. injection [Hakura et al., 1998; Monroe et al., 1998; Kosinska et al., 1999; Shane et al., 2000]. However, mutagenesis caused by the intratracheal instillation of B[*a*]P in the lung, the target organ of air pollutants, has not been analyzed quantitatively. Thus, it is very important to evaluate the mutagenicity of environmental carcinogens in the lung for evaluating the health risks of air pollution.

To evaluate the in vivo mutagenicity of B[*a*]P in the lung and to understand the relationship between the mutagenicity and carcinogenicity of B[*a*]P, we administered B[*a*]P directly into the lung of *gpt* delta mouse, a transgenic mouse for detecting in vivo mutations [Nohmi et al., 1996; Thybaud et al., 2003]. Although exposure to air pollutants should be ideally performed by inhalation [Mullin et al., 1998], administering B[*a*]P by inhalation is technically difficult. Thus, we decided to perform intratracheal instillation as a simple way of administering B[*a*]P into the lung. The *gpt* delta mouse is a transgenic mouse that carries lambda phage EG10 as a transgene for the determination of mutation. When the rescued phages are infected into *E. coli* expressing Cre recombinase, the phage DNA is converted into plasmids harboring the chloramphenicol (Cm)-resistance gene and the guanine phosphoribosyltransferase (*gpt*) gene. *gpt* mutants can be detected as colonies arising on plates containing Cm and 6-thioguanine (6-TG). The mutation assay using the *gpt* delta mouse was validated by demonstrating that the *gpt* transgene responds to mutagens in a manner similar to other transgenic loci, i.e., *lacZ* and *cII* [Swiger et al., 2001].

In this study, the mutant frequency and mutation spectrum in the lung *gpt* gene of *gpt* delta mouse were examined after intratracheal instillation of 0.5, 1, and 2 mg B[*a*]P per mouse. The present study shows that the lung *gpt* mutant and mutation frequency increased linearly with the dose of B[*a*]P instilled into the lungs. The predominant mutations induced by B[*a*]P were G:C→T:A transversions and deletions of single G:C base pairs.

MATERIALS AND METHODS

Treatment of Mice

Eleven male *gpt* delta mice (9 weeks old) were obtained from Japan SLC (Shizuoka, Japan). The mice carry approximately 80 copies of lambda EG10 DNA on each chromosome 17 on a C57BL/6J background [Nohmi et al., 1996]. B[*a*]P (Wako Pure Chemical Industries, Osaka, Japan) was dissolved in tricaprylin and given to each mouse in a single intratracheal instillation (three animals for 0.5 and 1 mg and two animals for 2 mg). The animals were anesthetized in a desiccator with 4% halothane (Hoechst Japan, Tokyo, Japan) until the animal did not respond to a tactile stimulus. The B[*a*]P solution was then instilled into the trachea via a polyethylene tube [Takano et al., 2002]. The 0.5 and 1 mg doses were dissolved in 50 μl tricaprylin ($[CH_3(CH_2)_6COOCH_2]_2$-$CHOCO(CH_2)_6CH_3$; Sigma-Aldrich, St. Louis, MO), and the 2 mg doses were dissolved in 100 μl tricaprylin. Three mice were treated with 50 μl tricaprylin alone as controls. The mice were sacrificed 14 days after B[*a*]P administration. Their lungs were removed, frozen in liquid nitrogen, and stored at −80°C until the DNA was isolated.

DNA Isolation and In Vitro Packaging of DNA

High-molecular-weight genomic DNA was extracted from the lungs using the RecoverEase DNA Isolation Kit (Stratagene, La Jolla, CA). Lambda EG10 phages were rescued using Transpack Packaging Extract (Stratagene).

gpt Mutation Assay

The *gpt* mutagenesis assay was performed according to previously described methods [Nohmi et al., 2000]. To convert the phage DNA into plasmids, *E. coli* YG6020 expressing Cre recombinase was infected with the rescued phage. The bacteria were then spread onto M9 salts plates containing Cm and 6-TG [Nohmi et al., 2000], which were incubated for 72 hr at 37°C for selection of the colonies harboring a plasmid carrying the chloramphenicol acetyltransferase (*cat*) gene and a mutated *gpt* gene. The 6-TG-resistant colonies were streaked onto selection plates for confirmation of the resistant phenotype. The cells were then cultured in LB broth containing 25 μg/ml of Cm at 37°C and collected by centrifugation. The bacterial pellets were stored at −80°C until DNA sequencing analysis was performed. Mutant frequencies for the *gpt* gene were calculated by dividing the number of colonies growing on M9 + Cm + 6-TG agar plates by the number of colonies growing on M9 + Cm agar plates.

PCR and DNA Sequencing Analysis of 6-TG-Resistant Mutants

A 739 bp DNA fragment containing the *gpt* gene was amplified by PCR using primer 1 (forward primer: 5′-TACCACTTTATCCCGCGTCAGG-3′) and primer 2 (reverse primer: 5′-ACAGGGTTTCGCTCAGGTTTGC-3′) [Nohmi et al., 2000]. The reaction mixture contained 5 pmole of each primer and 200 mM of each dNTP. PCR amplification was carried out using Ex Taq DNA polymerase (Takara Bio, Shiga, Japan) and performed with a Model PTC-100 Thermal Cycler (MJ Research, Waltham, MA). After the PCR products were purified, sequencing reactions were performed by using a DYEnamic ET Terminator kit (Amersham Biosciences, Piscataway, NJ). The sequencing primers were primer A (forward primer: 5′-GAGGCAGTGCGTAAAAAGAC-3′) and primer C (reverse primer: 5′-CTATTGTAACCCGCCTGAAG-3′) [Nohmi et al., 2000]. The sequencing reaction products were analyzed on an Applied Biosystems model 310 genetic analyzer (Applied Biosystems, Foster City, CA).

Statistical Analysis

All data are expressed as mean ± SD. Statistical significance was evaluated using ANOVA and the Scheffe test. $P < 0.05$ was considered to be statistically significant. To evaluate the linearity of the mutant frequency dose-response, a simple linear regression was performed. A statistical comparison of mutational spectra was performed using the Adams-Skopek test [Adams and Skopek, 1987; Cariello et al., 1994].

RESULTS

gpt Mutatnt Frequency in Lung of B[a]P-Treated Mice

To determine the mutagenic effects of B[*a*]P in the lung, *gpt* delta transgenic mice were exposed to increasing doses of B[*a*]P by intratracheal instillation. The body weights of mice given 0, 0.5, 1, and 2 mg B[*a*]P were 23.3 ± 0.9, 25.0 ± 0.0, 25.0 ± 0.6, and 24.5 ± 0.5 g, respectively, and there were no significant differences between the assay groups. The mutant frequency in the lungs of the control mice (0 mg B[*a*]P) was $0.60 \pm 0.13 \times 10^{-5}$ (n = 3). Single injections of 0.5, 1, and 2 mg resulted in increases in the mutant frequency of approximately 2.8-, 4.2-, and 6.8-fold ($1.7 \pm 0.22 \times 10^{-5}$, n = 3; $2.5 \pm 0.33 \times 10^{-5}$, n = 3; and 4.1×10^{-5}, n = 2), respectively, compared with the control mice (Table I). Mutation frequencies calculated from the mutant frequencies displayed similar fold increases. Significant differences were observed in the mutant and mutation frequencies between untreated and treated mice at the 1 and 2 mg doses but not at the 0.5 mg dose. The B[*a*]P treatment resulted in a significant linear dose-dependent increase in mutant frequency ($r^2 = 0.88$; $P < 0.001$; Fig. 1) and mutation frequency ($r^2 = 0.82$; $P < 0.01$; Fig. 1).

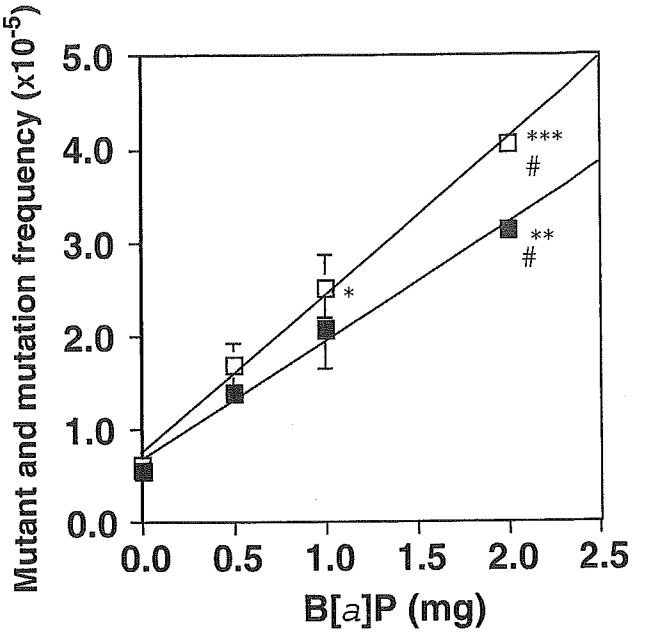

Fig. 1. 6-TG-induced mutant (open square) and mutation (filled square) frequency in the lungs of B[*a*]P-treated *gpt* delta mice. Data are expressed as mean ± SD (n = 3 for the control, 0.5 mg, and 1 mg groups; n = 2 for the 2 mg group). Number sign, average data of two animals. Statistical significance was determined using ANOVA and the Scheffe test. Significant differences between the control and B[*a*]P-induced groups are indicated: asterisk, $P < 0.05$; double asterisk, $P < 0.01$; triple asterisk, $P < 0.001$.

Characteristics of *gpt* Mutation Spectrum

To determine the spectrum of mutations caused by B[*a*]P instilled into the lung, 131 *gpt* mutants from the lungs of treated and control mice were subjected to DNA sequence analysis (Tables II and III). In control mice, 92% (12/13) of total mutations were base substitutions; G:C→C:G and G:C→T:A transversions and G:C→A:T transitions occurred at nearly equal frequencies. In the

TABLE II. Classification of *gpt* Mutations From the Lungs of Control and B[*a*]P-Treated Mice[a]

Type of mutation in the *gpt* gene	Control		B[*a*]P total[b]		B[*a*]P (mg) 0.5		1		2	
	Total/ independent	%/% independent	Total/ independent	%/% independent	Total/ independent	%/% independent	Total/ independent	%/% independent	Total/ independent	%/% independent
Base substitution										
Transition										
G:C→A:T	3/3	23/25	13/11	11/13	3/2	23/20	4/4	10/14	6/5	10/10
(at CpG site)	(1/1)		(6/4)		(2/1)		(1/1)		(3/2)	
A:T→G:C	2/2	15/17	3/2	3/2	1/1	8/10	0	0	2/1	3/2
Transversion										
G:C→T:A	3/3	23/25	52/30	44/34	6/4	46/40	23/11	55/38	23/15	37/31
G:C→C:G	4/3	31/25	13/13	11/15	1/1	8/10	7/7	17/24	5/5	8/10
A:T→T:A	0	0	8/4	7/5	0	0	0	0	8/4	13/8
A:T→C:G	0	0	0	0	0	0	0	0	0	0
Deletion										
−1	1/1	8/8	16/15	14/17	2/2	15/20	4/4	10/14	10/9	16/19
>2	0	0	2/2	2/2	0	0	0	0	2/2	3/4
Insertion	0	0	9/8	8/9	0	0	2/1	5/3	7/7	11/15
Other	0	0	2/2	2/2	0	0	2/2	5/7	0	0
Total	13/12		118/87		13/10		42/29		63/48	

[a]Independent mutations were isolated no more than once from any individual mouse.
[b]Mutations combined from all treatment doses.

TABLE III. DNA Sequence Analysis of *gpt* Mutations Obtained From the Lung of B[*a*]P-Treated and Untreated Control *gpt* delta Mice

Type of mutation	Nucleotide	Sequence change		Amino acid change	Total number of mutants (independent)[a]		Number of mutants									
							Control			B[*a*]P 0.5 mg			B[*a*]P 1 mg			B[*a*]P 2 mg	
					Control	B[*a*]P	Number 1	Number 2	Number 3	Number 1	Number 2	Number 3	Number 1	Number 2	Number 3	Number 1	Number 2
Base substitution																	
Transition																	
G:C→A:T	64	Cga→Tga	CpG	Arg→Stop		2 (1)						2					
	86	tGg→tAg		Trp→Stop		2								1		1	
	110	cGt→cAt	CpG	Arg→His	1	3 (2)	1									1	2
	115	Ggt→Agt	CpG	Gly→Ser		1								1			
	128	gGt→gAt		Gly→Asp		1										1	
	262	Gat→Aat		Asp→Asn	1				1								
	274	Gat→Aat		Asp→Asn	1			1									
	352	Ggt→Agt		Gly→Ser		1										1	
	402	tgG→tgA		Trp→Stop		1									1		
	409	Cag→Tag		Gln→Stop		1						1					
	418	Gat→Aat		Asp→Asn		1							1				
A:T→G:C	25	Tgg→Cgg		Trp→Arg	1			1									
	56	cTc→cCc		Leu→Pro	1	1		1			1						
	415	Tgg→Cgg		Trp→Arg		2 (1)										2	
Transversion																	
G:C→T:A	7	Gaa→Taa	CpG	Glu→Stop		3 (1)				3							
	108	agC→agA		Ser→Arg		2 (1)									2		
	110	cGt→cTt	CpG	Arg→Leu		3 (2)										2	1
	115	Ggt→Tgt	CpG	Gly→Cys		4 (3)									2	1	1
	116	gGt→gTt		Gly→Val		1				1							
	140	gCg→gAg	CpG	Ala→Glu		3									1	1	1
	143	cGt→cTt	CpG	Arg→Leu		10 (4)							1		7	1	1
	176	tGt→tTt		Cys→Phe		1											1
	185	aGc→aTc		Ser→Ile	1		1										
	186	agC→agA		Ser→Arg	1			1									
	189	taC→taA	CpG	Tyr→Stop		4 (3)							2		1		1
	208	Gag→Tag	CpG	Glu→Stop		4 (2)									3		1
	244	Gaa→Taa	CpG	Glu→Stop		10 (2)									2		8
	304	Gaa→Taa		Glu→Stop	1	1			1	1							
	402	tgG→tgT		Trp→Cys		2								1			1
	409	Cag→Aag		Gln→Lys		1										1	
	413	cCg→cAg	CpG	Pro→Gln		3				1					1	1	
G:C→C:G	50	cGt→cCt	CpG	Arg→Pro		1									1		
	108	agC→agG		Ser→Arg		1										1	
	112	Ggc→Cgc		Gly→Arg	1		1										
	125	cCg→cGg	CpG	Pro→Arg		2							1		1		
	143	cGt→cCt	CpG	Arg→Pro		1											1
	186	agC→agG		Ser→Arg	2 (1)	1	2								1		
	206	cGc→cCc	CpG	Arg→Pro		1										1	

(*Continued*)

TABLE III. *Continued*

Type of mutation	Nucleotide	Sequence change		Amino acid change	Total number of mutants (independent)[a]		Number of mutants										
					Control		Control			B[*a*]P 0.5 mg			B[*a*]P 1 mg			B[*a*]P 2 mg	
							Number 1	Number 2	Number 3	Number 1	Number 2	Number 3	Number 1	Number 2	Number 3	Number 1	Number 2
	280	Ggt→Cgt	CpG	Gly→Arg		1									1		
	289	Gcg→Ccg		Ala→Pro		1							1				
	340	Gca→Cca	CpG	Ala→Pro	1	2			1					1		1	
	413	cCg→cGg	CpG	Pro→Arg		1						1					
	418	Gat→Cat		Asp→His		1										1	
A:T→T:A	35	tTg→tAg		Leu→Stop		1										1	
	146	gAa→gTa		Glu→Val		1										1	
	254	aTc→aAc		Ile→Asn		1											1
	415	Tgg→Agg		Trp→Arg		5 (1)										5	
Deletion																	
−1 base	8-12	AAAAA→AAAA			1			1									
	23-24	aCCt→aCt				1											1
	93	gCa→ga				1										1	
	103	cGta→cta				1											1
	115-116	cGGt→cGt				1											1
	120-121	tGGt→tGt				2 (1)											2
	150-152	tGGGt→tGGt				1										1	
	170-171	aCCg→aCg				1											1
	173-175	gTTTg→gTTg				1											1
	198	aCa→aa				1							1				
	237	gCg→gg				1				1							
	244	cGa→ca				1									1		
	270-271	tGGt→tGt				1									1		
	283-284	tGGt→tGt				1										1	
	416-418	tGGGa→tGGa				1						1					
	442-443	gCCa→gCa				1									1		
> 2 base	173-179	gTTTGTATt→gt				1											1
	226-227	aCGc→ac				1										1	
Insertion																	
	60-61	CAAG→CAAAG				1											1
	62	AGC→ACGC				1											1
	132	CGT→CAGT				1										1	
	188	TAC→TAAC				1										1	
	280-281	CCGGT→CCGGGT				1										1	
	351	CTG→CATG				1										1	
	392-393	CAAG→CAAAG				1										1	
	401-402	TGGA→TGGGA				2 (1)									2		
Other																	
	26-27	TGGGA→TTGA				1							1				
	140-141	GGCGC→GGAAC				1									1		

[a]Mutations isolated more than once from a single mouse assumed to be siblings and counted only once.

B[*a*]P-treated group, 44% of the mutations (52/118) were G:C→T:A transversions, and 14% (16/118) were one-base deletions. A dose-dependent increase in base deletions was observed in the range of 0–2 mg B[*a*]P, while G:C→T:A transversions increased with dose at 0.5–1 mg B[*a*]P, but decreased slightly at 2 mg B[*a*]P.

The mutational analysis data were used to estimate mutation frequency. Mutations that were isolated more than once from an individual mouse were considered to be the result of clonal expansion and counted as a single independent mutation. Using this correction, 92% (12/13) of control mutations were independent, while 74% (87/118) of mutations from treated mice were independent. For most types of mutations, independent mutations and total mutations displayed very similar distributions (Table II), and mutant frequency and mutation frequency had very similar dose-response relationships (Fig. 1, Table I). Marked differences between mutant frequency and mutation frequency, however, were observed for G:C→T:A transversions. The mutant frequency for G:C→T:A transversion was estimated to be 0.11×10^{-5} (control), 0.61×10^{-5} (0.5 mg B[*a*]P), 1.4×10^{-5} (1 mg B[*a*]P), and 1.3×10^{-5} (2 mg B[*a*]P), as shown in Figure 2. On the other hand, the mutation frequency for G:C→T:A transversion was estimated to be 0.11, 0.41, 0.69, and 0.82×10^{-5} for 0, 0.5, 1, and 2 mg of B[*a*]P, respectively. Although different, both the mutation frequency and mutant frequency for G:C→T:A transversion increased dose-dependently.

There was a significant difference between the mutation spectra shown in Table II for untreated mice and mice treated with 1 mg B[*a*]P ($P < 0.05$). The spectra for mice treated with 0.5 and 2 mg B[*a*]P, however, were not significantly different from the control spectrum ($P = 0.60$ and 0.056). Also, there was no significant difference between the control mutation spectrum and the spectrum of total B[*a*]P-induced mutations ($P = 0.10$) or between the spectrum of independent control mutations and either the spectrum of total B[*a*]P-induced independent mutations ($P = 0.09$) or the spectrum of independent mutations produced by each of the different doses of B[*a*]P ($P = 0.86$, 0.30, and 0.15).

The positions of *gpt* mutations induced by B[*a*]P are listed in Table III. Among the G:C→T:A transversions isolated from B[*a*]P-treated mice, five *gpt* mutations (at nucleotides 115, 140, 143, 189, and 413) were each observed in three or more mice; these positions therefore are potential hotspots for B[*a*]P mutation. Significant differences were observed for the hotspots in untreated and treated mice ($P < 0.05$, Adams-Skopek test).

The predominant frameshift mutation in B[*a*]P-treated mice was single-base pair deletion of G:C base pairs (15/16; 94%). Thirty-eight percent of single-base deletions (6/16) occurred at G:C sites in 5′-TGG-3′ sequences, and the deletion of G:C from a run of G:Cs occurred in 63% of −1 frameshifts (10/16; Table III). There were, however, no apparent hotspots for deletion.

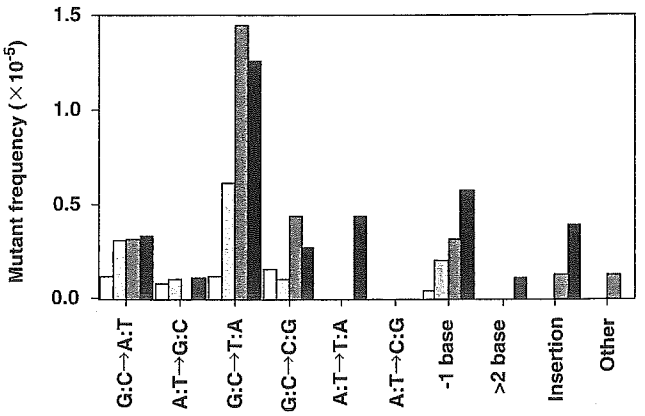

Fig. 2. Comparison of 6-TG-induced mutation spectra (not corrected for clonality) in control and B[*a*]P-treated *gpt* delta mice. Open bar, control; light gray bar, 0.5 mg; dark gray bar, 1 mg; closed bar, 2 mg.

DISCUSSION

To determine the mutant frequency and mutation spectrum induced by B[*a*]P in the lung, B[*a*]P was administered directly into the lungs of *gpt* delta mice. The mutagenicity of B[*a*]P has previously been determined in the liver, spleen, forestomach, and bone marrow using oral administration or i.p. injection in the Big Blue mouse [Skopek et al., 1996; Shane et al., 1997, 2000], Muta Mouse [Mientjes et al., 1996; Rompelberg et al., 1996; Hakura et al., 1998; Kosinska et al., 1999], and the *rpsL* transgenic mouse [Muto et al., 1999]. In these reports, the authors did not determine whether the mutant frequency depended on the dose of B[*a*]P except for one study using spleen T-cells [Skopek et al., 1996]. Our results indicate that the mutant frequency in the lung increases linearly with the dose of B[*a*]P. Therefore, when this compound is directly administered to a target organ, the lung, the amount of B[*a*]P bound to DNA in the form of a BPDE-DNA adduct appears to be proportional to the dose of B[*a*]P administered.

B[*a*]P administered by intratracheal injection also causes lung tumors in direct proportion to the total dose (0–8 mg) [Yoshimoto et al., 1983; Ide et al., 2000; Tchou-Wong et al., 2002]. For instance, the incidence of lung tumors was 39% at a dose of 4 mg B[*a*]P [Tchou-Wong et al., 2002]. These data indicate that lung tumors are induced under the same conditions and with a similar dose response as *gpt* mutations in *gpt* delta mice. Human B[*a*]P intake from air was estimated by Raiyani et al. [1993]. On the basis of an average inhalation of 15 m^3 air per day, exposure to B[*a*]P was calculated to be 0.19 μg/day in industrial areas [International Programme on Chemical Safety, 1998]. Therefore, the 1 mg dose of B[*a*]P used in this report is equivalent to the total intake of B[*a*]P received through inhalation over 14.4 years (5,263 days).

To analyze the spectrum of mutations caused by B[*a*]P in the lung, we determined the sequences of mutated *gpt* genes.

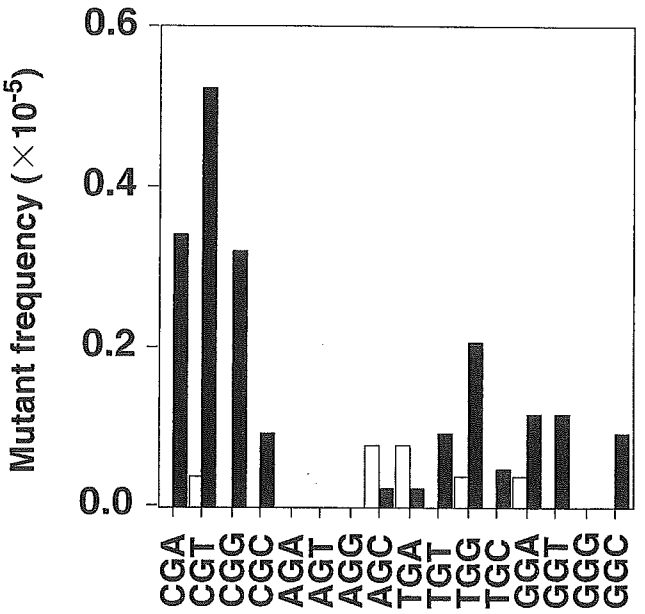

Fig. 3. Sequence dependence of B[*a*]P-induced mutations in the *gpt* gene. Open bar, control; closed bar, B[*a*]P-induced. Frequencies not corrected for clonality.

The predominant B[*a*]P-induced mutations in the *gpt* gene were single-base substitutions and deletions and these occurred mainly at G:C base pairs (Fig. 2, Tables II and III). The major types of base substitutions were G:C→T:A transversions, followed by G:C→C:G transversions and G:C→A:T transitions. Hakura et al. [2000] reported that G:C→T:A transversions are the major mutation in forestomach (55%) and in spleen (50%) of Muta Mouse following oral administration of B[*a*]P. G:C→T:A transversions are also the major type of base substitution in the liver (31.8%) of Big Blue mice following i.p. injection of B[*a*]P [Shane et al., 2000]. In these reports, base deletions caused by B[*a*]P were only a minor component. However, Yamada et al. [2002] reported that gavage treatment of Muta Mouse with B[*a*]P resulted in not only G:C→T:A transversions but also deletions of single G:C base pairs in the liver and the frequency (5/36; 14%) was similar to the G:C deletion frequency found in the present study (16/118; 14%).

Our results indicate that the frequency of G:C→T:A transversion mutants increases at doses of 0.5 and 1 mg B[*a*]P, but was slightly decreased at a dose of 2 mg B[*a*]P. The frequency of base deletion also increased with the dose of B[*a*]P (Fig. 2). At 2 mg B[*a*]P, A:T→T:A transversions and insertion mutations occurred along with G:C→T:A transversions and deletions, indicating that B[*a*]P may cause a different spectrum of mutations at high doses (Fig. 2, Table II). At 1 mg of B[*a*]P, the mutation spectrum (not corrected for independence) was significantly different between the treated group and the control group by the Adams-Skopek test. However, at a dose of 2 mg, there was no significant difference in the mutation spectrum.

In control mice, 92% (12/13) of the total mutations were base-substitution mutations: G:C→C:G and G:C→T:A transversions and G:C→A:T transitions. This observation is somewhat different from a previous report showing that spontaneous 6-TG-resistant mutations in other tissues of *gpt* delta mice are predominantly G:C→A:T transitions [Masumura et al., 2000]. The possibility that the tricaprylin vehicle caused the transversions cannot be ruled out. However, the mutant frequency of control mice in this study is the same as the frequency observed previously in other tissues of *gpt* delta mice [Masumura et al., 1999, 2003], suggesting that tricaprylin has no substantial influence on mutagenesis and that the difference in spectra may be a result of the relatively few spontaneous mutant analyzed. The relatively few control mutations isolated in this study may also have compromised attempts to establish differences in mutational spectra between control and B[*a*]P-treated mice.

An analysis of sequences adjacent to the mutated guanine base (Fig. 3) identified the nucleotide sequences CGT, CGA, and CGG in the *gpt* gene as major targets of B[*a*]P. The mutation spectra (mutations at these guanine bases) were significantly different between untreated and treated mice ($P = 0.002$, Adams-Skopek test). Similar G:C sites are also targets of B[*a*]P mutagenesis in the Muta Mouse and Big Blue mouse [Hakura et al., 2000; Shane et al., 2000]. Denissenko et al. [1996] reported that the BPDE mutation spectrum in the tumor suppressor gene *p53* was characterized by hotspots at G:C sites at nucleotides 157 (CGT), 248 (CGG), and 273 (CGT). Thus, CGT and CGG are target sites of B[*a*]P in endogenous genes as well as in the transgene *gpt*, suggesting that analyzing the mutation spectrum in a transgene can play an important role in identifying the target sequences of a mutagen in an endogenous gene. Our results thus provide useful information regarding in vivo mutations caused by B[*a*]P in the lung, an organ that is affected by the inhalation of air pollution.

ACKNOWLEDGMENTS

The authors thank Dr. Osami Nakasugi, Dr. Michi Matsumoto, and Dr. Wakae Maruyama for support and advice.

REFERENCES

Adams WT, Skopek TR. 1987. Statistical test for the comparison of samples from mutational spectra. J Mol Biol 194:391–396.

Bartsch H. 1996. DNA adducts in human carcinogenesis: etiological relevance and structure-activity relationship. Mutat Res 340:67–79.

Buening MK, Wislocki PG, Levin W, Yagi H, Thakker DR, Akagi H, Koreeda M, Jerina DM, Conney AH. 1978. Tumorigenicity of the optical enantiomers of the diastereomeric benzo[*a*]pyrene 7,8-diol-9,10-epoxides in newborn mice: exceptional activity of (+)-7β,8α-dihydroxy-9α,10α-epoxy-7,8,9,10-tetrahydrobenzo[*a*]-pyrene. Proc Natl Acad Sci USA 75:5358–5361.

Cariello NF, Piegorsch WW, Adams WT, Skopek TR. 1994. Computer program for the analysis of mutational spectra: application to *p53* mutations. Carcinogenesis 15:2281–2285.

Cohen GM, Haws SM, Moore BP, Bridges JW. 1976. Benzo(a)pyren-3-yl hydrogen sulphate, a major ethyl acetate-extractable metabolite of benzo(a)pyrene in human, hamster and rat lung cultures. Biochem Pharmacol 25:2561–2570.

Cosman M, de los Santos C, Fiala R, Hingerty BE, Singh SB, Ibanez V, Margulis LA, Live D, Geacintov NE, Broyde S. 1992. Solution conformation of the major adduct between the carcinogen (+)-anti-benzo[*a*]pyrene diol epoxide and DNA. Proc Natl Acad Sci USA 89:1914–1918.

Denissenko MF, Pao A, Tang MS, Pfeifer GP. 1996. Preferential formation of benzo[*a*]pyrene adducts at lung cancer mutational hotspots in P53. Science 274:430–432.

Hakura A, Tsutsui Y, Sonoda J, Kai J, Imade T, Shimada M, Sugihara Y, Mikami T. 1998. Comparison between in vivo mutagenicity and carcinogenicity in multiple organs by benzo[*a*]pyrene in the *lacZ* transgenic mouse (Muta Mouse). Mutat Res 398:123–130.

Hakura A, Tsutsui Y, Sonoda J, Tsukidate K, Mikami T, Sagami F. 2000. Comparison of the mutational spectra of the *lacZ* transgene in four organs of the Muta Mouse treated with benzo[*a*]pyrene: target organ specificity. Mutat Res 447:239–247.

Ide F, Iida N, Nakatsuru Y, Oda H, Tanaka K, Ishikawa T. 2000. Mice deficient in the nucleotide excision repair gene *XPA* have elevated sensitivity to benzo[*a*]pyrene induction of lung tumors. Carcinogenesis 21:1263–1265.

International Programme on Chemical Safety. 1998. Selected non-heterocyclic polycyclic aromatic hydrocarbons: environmental health criteria 202.Geneva:World Health Organization. p267–276.

Iwagawa M, Maeda T, Izumi K, Otsuka H, Nishifuji K, Ohnishi Y, Aoki S. 1989. Comparative dose-response study on the pulmonary carcinogenicity of 1,6-dinitropyrene and benzo[*a*]pyrene in F344 rats. Carcinogenesis 10:1285–1290.

Kosinska W, von Pressentin MdM, Guttenplan JB. 1999. Mutagenesis induced by benzo[*a*]pyrene in *lacZ* mouse mammary and oral tissues: comparisons with mutagenesis in other organs and relationships to previous carcinogenicity assays. Carcinogenesis 20: 1103–1106.

Masumura K, Matsui K, Yamada M, Horiguchi M, Ishida K, Watanabe M, Ueda O, Suzuki H, Kanke Y, Tindall KR, Wakabayashi K, Sofuni T, Nohmi T. 1999. Mutagenicity of 2-amino-1-methyl-6-phenylimidazo [4,5-*b*]pyridine (PhIP) in the new *gpt* delta transgenic mouse. Cancer Lett 143:241–244.

Masumura K, Matsui K, Yamada M, Horiguchi M, Ishida K, Watanabe M, Wakabayashi K, Nohmi T. 2000. Characterization of mutations induced by 2-amino-1-methyl-6-phenylimidazo[4,5-*b*]pyridine in the colon of *gpt* delta transgenic mouse: novel G:C deletions beside runs of identical bases. Carcinogenesis 21:2049–2056.

Masumura K, Horiguchi M, Nishikawa A, Umemura T, Kanki K, Kanke Y, Nohmi T. 2003. Low dose genotoxicity of 2-amino-3,8-dimethylimidazo-[4,5-*f*]quinoxaline (MeIQx) in *gpt* delta transgenic mice. Mutat Res 541:91–102.

Mientjes EJ, Steenwinkel MJST, van Delft JHM, Lohman PHM, Baan RA. 1996. Comparison of the X-gal- and P-gal-based systems for screening of mutant λ *lacZ* phages originating from the transgenic mouse strain 40.6. Mutat Res 360:101–106.

Miller ML, Vasunia K, Talaska G, Andringa A, de Boer J, Dixon K. 2000. The tumor promoter TPA enhances benzo[*a*]pyrene and benzo[*a*]pyrene diolepoxide mutagenesis in Big Blue mouse skin. Environ Mol Mutagen 35:319–327.

Monroe JJ, Kort KL, Miller JE, Marino DR, Skopek TR. 1998. A comparative study of in vivo mutation assays: analysis of *hprt*, *lacI*, and *cII/cI* as mutational targets for *N*-nitroso-*N*-methylurea and benzo[*a*]pyrene in Big Blue mice. Mutat Res 421:121–136.

Mullin AH, Nataraj D, Ren JJ, Mullin DA. 1998. Inhaled benzene increases the frequency and length of *lacI* deletion mutations in lung tissues of mice. Carcinogenesis 19:1723–1733.

Muto S, Yokoi T, Gondo Y, Katsuki M, Shioyama Y, Fujita K, Kamataki T. 1999. Inhibition of benzo[*a*]pyrene-induced mutagenesis by (−)-epigallocatechin gallate in the lung of *rpsL* transgenic mice. Carcinogenesis 20:421–424.

Nohmi T, Katoh M, Suzuki H, Matsui M, Yamada M, Watanabe M, Suzuki M, Horiya N, Ueda O, Shibuya T, Ikeda H, Sofuni T. 1996. A new transgenic mouse mutagenesis test system using Spi$^-$ and 6-thioguanine selections. Environ Mol Mutagen 28: 465–470.

Nohmi T, Suzuki T, Masumura K. 2000. Recent advances in the protocols of transgenic mouse mutation assays. Mutat Res 455:191–215.

Prough RA, Patrizi VW, Okita RT, Masters BSS, Jakobsson SW. 1979. Characteristics of benzo(a)pyrene metabolism by kidney, liver and lung microsomal fractions from rodents and humans. Cancer Res 39:1199–1206.

Raiyani CV, Jani JP, Desai NM, Shah JA, Kashyap SK. 1993. Levels of polycyclic aromatic hydrocarbons in ambient environment of Ahmedabad City. Ind J Environ Prot 13:206–215.

Rompelberg CJM, Steenwinkel MJST, van Asten JG, van Delft JHM, Baan RA, Verhagen H. 1996. Effect of eugenol on the mutagenicity of benzo[*a*]pyrene and the formation of benzo[*a*]pyrene-DNA adducts in the λ-*lacZ*-transgenic mouse. Mutat Res 369: 87–96.

Shane BS, Lockhart AMC, Winston GW, Tindall KR. 1997. Mutant frequency of *lacI* in transgenic mice following benzo[*a*]pyrene treatment and partial hepatectomy. Mutat Res 377:1–11.

Shane BS, de Boer J, Watson DE, Haseman JK, Glickman BW, Tindall KR. 2000. *LacI* mutation spectra following benzo[*a*]pyrene treatment of Big Blue mice. Carcinogenesis 21:715–725.

Singh SV, Benson PJ, Hu X, Pal A, Xia H, Srivastava SK, Awasthi S, Zaren HA, Orchard JL, Awasthi YC. 1998. Gender-related differences in susceptibility of A/J mouse to benzo[*a*]pyrene-induced pulmonary and forestomach tumorigenesis. Cancer Lett 128:197–204.

Skopek TR, Kort KL, Marino DR, Mittal LV, Umbenhauer DR, Laws GM, Adams SP. 1996. Mutagenic response of the endogenous *hprt* gene and *lacI* transgene in benzo[*a*]pyrene-treated Big Blue B6C3F1 mice. Environ Mol Mutagen 28:376–384.

Swiger RR, Cosentino L, Masumura K, Nohmi T, Heddle JA. 2001. Further characterization and validation of *gpt* delta transgenic mice for quantifying somatic mutations in vivo. Environ Mol Mutagen 37:297–303.

Takano H, Yanagisawa R, Ichinose T, Sadakane K, Inoue K, Yoshida S, Takeda K, Yoshino S, Yoshikawa T, Morita M. 2002. Lung expression of cytochrome P450 1A1 as a possible biomarker of exposure to diesel exhaust particles. Arch Toxicol 76:146–151.

Tchou-Wong KM, Jiang Y, Yee H, LaRosa J, Lee TC, Pellicer A, Jagirdar J, Gordon T, Goldberg JD, Rom WN. 2002. Lung-specific expression of dominant-negative mutant p53 in transgenic mice increases spontaneous and benzo(a)pyrene-induced lung cancer. Am J Respir Cell Mol Biol 26:186–193.

Thybaud V, Dean S, Nohmi T, de Boer J, Douglas GR, Glickman BW, Gorelick NJ, Heddle JA, Heflich RH, Lambert I, Martus HJ, Mirsalis JC, Suzuki T, Yajima N. 2003. In vivo transgenic mutation assays. Mutat Res 540:141–151.

Yamada K, Suzuki T, Kohara A, Hayashi M, Hakura A, Mizutani T, Saeki K. 2002. Effect of 10-aza-substitution on benzo[*a*]pyrene mutagenicity in vivo and in vitro. Mutat Res 521:187–200.

Yoshimoto T, Inoue T, Iizuka H, Nishikawa H, Sakatani M, Ogura T, Hirao F, Yamamura Y. 1980. Differential induction of squamous cell carcinomas and adenocarcinomas in mouse lung by intratracheal instillation of benzo(a)pyrene and charcoal powder. Cancer Res 40:4301–4307.

In Vivo Mutational Analysis of Liver DNA in *gpt* Delta Transgenic Rats Treated With the Hepatocarcinogens *N*-Nitrosopyrrolidine, 2-Amino-3-Methylimidazo[4,5-*f*]Quinoline, and Di(2-Ethylhexyl)Phthalate

Keita Kanki,[1] Akiyoshi Nishikawa,[1]* Ken-ichi Masumura,[2] Takashi Umemura,[1] Takayoshi Imazawa,[1] Yasuki Kitamura,[1] Takehiko Nohmi,[2] and Masao Hirose[1]

[1]*Division of Pathology, National Institute of Health Sciences, Setagaya-ku, Tokyo, Japan*
[2]*Division of Genetics and Mutagenesis, National Institute of Health Sciences, Setagaya-ku, Tokyo, Japan*

In order to cast light on carcinogen-specific molecular mechanisms underlying experimental hepatocarcinogenesis in rats, in vivo mutagenicity and mutation spectra of known genotoxic rat hepatocarcinogens *N*-nitrosopyrrolidine (NPYR), and 2-amino-3-methylimidazo[4,5-*f*]quinoline (IQ), as well as the nongenotoxic hepatocarcinogen di(2-ethylhexyl)phthalate (DEHP) and the noncarcinogen acetaminophen (AAP), were investigated in guanine phosphoribosyltransferase (*gpt*) delta transgenic rats, a recently developed animal model for genotoxicity analysis. After 13-wk treatment, glutathione *S*-transferase placental form (GST-P)-positive liver cell foci were significantly increased in NPYR-treated and IQ-treated rats. In the DEHP-treated rats, marked hepatomegaly with centrilobular hypertrophy of hepatocytes occurred, although GST-P staining was consistently negative. Positive mutagenicity was detected in IQ- and NPYR-treated rats. Mutant frequencies (MFs) in the liver DNA were 188.0×10^{-6} and 56.5×10^{-6}, approximately 35-fold and 10-fold higher, respectively, than that of nontreatment control rats (5.5×10^{-6}). There were no increases in MFs in the DEHP- or AAP-treated rats as compared to the nontreatment control value. IQ induced mainly base substitutions leading to G:C to T:A transversions (56.9%) and deletions of G:C base pairs. In contrast, NPYR primarily caused specific A:T to G:C transitions (49.3%), which are very rare in the other groups. These data provided support for the conclusion that IQ and NPYR hepatocarcinogenesis depends on genotoxic processes and specific DNA adduct formation while DEHP exerts its influence via a nongenotoxic promotional pathway. Our data also indicate that analysis of specific in vivo mutational responses with transgenic animal models can provide crucial information for understanding the molecular mechanisms underlying chemical carcinogenesis. © 2004 Wiley-Liss, Inc.

Key words: hepatocarcinogens; in vivo mutation assay; *gpt* delta rats

INTRODUCTION

Environmental carcinogens are classified into genotoxic and nongenotoxic types based on in vitro bacterial mutagenicity. However, it is well-documented that in vitro mutagenicity does not always reflect in vivo mutagenicity and carcinogenicity in rodents [1–4]. The discrepancy between in vivo and in vitro models may result from organ-specific pathways of xenobiotic metabolism and DNA repair in vivo. To accomplish in vivo detection of gene mutations in multiple organs, transgenic rodents carrying reporter genes such as *lacI*, *lacZ*, and guanine phosphoribosyltransferase (*gpt*) have been developed [5]. These model animals can provide crucial information for understanding the in vivo mechanism of organ-specific mutagenesis induced by various carcinogens present in the human environment.

In spite of the toxicological importance of rat species, in vivo mutagenicity has been extensively studied in transgenic mice because of their availability. Recently, a novel transgenic rodent for genotoxicity analysis, named the *gpt* delta rat, has been developed [6]. Advantageous features allow positive detection of different types of mutations, including point mutations and deletions, as also shown with *gpt* delta mice [7]. Point mutations are

Abbreviations: *gpt*, guanine phosphoribosyltransferase; 6-TG, 6-thioguanine; NPYR, *N*-nitrosopyrrolidine; IQ, 2-amino-3-methylimidazo[4,5-*f*]quinoline; DEHP, di(2-ethylhexyl)phthalate; AAP, acetaminophen; MEHP, mono(2-ethylhexyl)phthalate; 8-OHdG, 8-hydroxydeoxyguanosine; MF, mutant frequency; GST-P, glutathione *S*-transferase placental form.

*Correspondence to: Division of Pathology, National Institute of Health Sciences, 1-18-1 Kamiyoga, Setagaya-ku, Tokyo 158-8501, Japan.

Received 21 May 2004; Revised 22 July 2004; Accepted 24 August 2004

DOI 10.1002/mc.20061

Published online 15 October 2004 in Wiley InterScience (www.interscience.wiley.com)

detected by 6-thioguanine (6-TG) selection with the *gpt* gene of *E. coli* and deletion mutations are identified by Spi$^-$ selection with the *red/gam* genes of lambda phage [5]. In the present study, aimed at elucidating carcinogen-specific mutagenic mechanisms underlying experimental hepatocarcinogenesis, in vivo mutation spectrum of *N*-nitrosopyrrolidine (NPYR), a carcinogenic cyclic nitrosamine present in processed food and tobacco smoke in the human environment [8,9], was investigated in *gpt* delta rats. NPYR is metabolically activated by microsomal P450, and its metabolites have been shown to form guanine adducts mainly, due to simple alkylation in the in vitro system [10]. The in vitro mutagenicity is detected only in the presence of an activating system such as rat liver homogenate [11]. Although the bacterial systems with *lacI* gene and M13mp2 phage DNA have shown the predominant base substitutions at G:C base pair [12,13], the in vivo mutation spectrum of NPYR has not yet been determined. Therefore, with *gpt* delta rats, the present study aimed to elucidate the in vivo mechanism of mutagenesis induced by NPYR in comparison with the mutation spectra of other hepatocarcinogens. For this purpose, well-studied rodent hepatocarcinogens 2-amino-3-methylimidazo[4,5-*f*]quinoline (IQ) and di(2-ethylhexyl)phthalate (DEHP) were also subjected to the in vivo mutation assay. In addition, a nonmutagenic hepatotoxic compound, acetaminophen (AAP), was used as a negative control chemical for the mutagenicity assay.

Heterocyclic aromatic amines are the major class of genotoxic hepatocarcinogens in rodents, as well as *N*-nitroso compounds, which may be active in humans [14,15]. IQ is one of the most carcinogenic and mutagenic heterocyclic aromatic amine present in cooked-foods and cigarette smoke [14,16]. In rodents, it exerts multipotential carcinogenicity in various organs [17], including the liver of nonhuman primates [18]. Potent mutagenicity with DNA adduct formation has been shown both in vitro and in vivo [19] and mutational analysis conducted in BigBlue rats has revealed characteristic G:C transversions and 1 bp G:C deletions in the liver, colon, and kidney [20]. Thus, because of abundant background data of carcinogenicity and mutagenicity, IQ can be used as an appropriate standard mutagen for the mutational analysis.

DEHP is a widely used plasticizer for vinylchloride products, which has been found to cause liver tumors in rats and mice in long-term feeding assays [21]. Because no mutagenicity has been detected in in vitro mutagenicity tests [22,23], DEHP has been categorized as a nongenotoxic carcinogen. However, several studies have suggested possible mutagenicity of mono(2-ethylhexyl)phthalate (MEHP), a principal hydrolysis metabolite of DEHP, in the reverse mutation assay (*E. coli*) and the Rec$^-$ assay (*B. subtilis*) [24,25]. Moreover, significant increases of 8-hydroxydeoxyguanosine (8-OHdG), a premutagenic DNA adduct formed by oxidative stress, have been observed in hepatic DNA of rats treated with DEHP, suggesting the involvement of oxidative DNA damage in its hepatocarcinogenesis [26,27]. Thus, in the present study DEHP was included in order to clarify its in vivo mutagenicity in the *gpt* delta system, which can widely and efficiently detect both point mutations and deletions with two different types of selection.

Accumulated studies have suggested that the transgenic animals are useful models for evaluating carcinogenic risk and chemopreventive potential of environmental materials to which humans are exposed [28–30]. Moreover, analyses of mutation spectra provide important information for understanding the molecular mechanisms underlying chemical carcinogenesis [31]. In the present study, in vivo mutagenicity analyses of major classes of rodent hepatocarcinogens were, therefore, performed in *gpt* delta rats and their possible mechanisms of hepatocarcinogenesis are discussed.

MATERIALS AND METHODS

Animals and Treatments

Twenty-five female Sprague-Dawley *gpt* delta rats carrying about ten tandem copies of the transgene lambda EG10 per haploid genome obtained from Japan SLC (Shizuoka, Japan) were randomized by weight into five groups. They were housed in a room with a barrier system, and maintained under the following constant conditions: temperature of 24 ± 1°C, relative humidity of 55 ± 5%, ventilation frequency of 18 times/h, and a 12 h light-dark cycle with free access to Oriental MF basal diet (Oriental Yeast Co., Ltd., Tokyo, Japan) and tap water.

Starting at 11-wk of age the rats were treated with test chemicals or maintained as controls for 13 wk. Groups of five animals were fed IQ (Toronto Research Chemical, Inc., Ont., Canada), DEHP (Wako Pure Chemical, Osaka, Japan), and AAP (Sigma Chemical Co., St. Louis, MO) at doses of 300, 12000, and 10000 ppm in MF basal diet, respectively. Another five rats were given NPYR (Aldrich Chemical Co., Milwaukee, WI) dissolved in a small quantity of ethanol and diluted in their drinking water at a dose of 200 ppm. The five nontreatment control rats received MF basal diet alone and tap water. At the end of the experiment, all animals were killed, and a part of the left lateral lobe of the liver was preserved at −80°C for subsequent in vivo mutation assays. The rest of the lobes were fixed in 10% buffered formalin for histopathological examination. Immunostaining of glutathione *S*-transferase placental form (GST-P) was performed by using polyclonal anti-GST-P (MBL, Nagoya, Japan) as the primary antibody, and goat IgG raised against rabbit

IgG as the secondary antibody. The signals were amplified with ABC KIT (DAKO, Kyoto, Japan), and detected with 3,3′-diaminobenzidine (DAB). The numbers and areas of GST-P positive liver cell foci comprising ten or more cells were measured by using an Image Processor for Analytical Pathology (IPAP, Sumika Technos, Osaka, Japan).

In Vivo Mutation Assays

The 6-TG and Spi$^-$ selections were performed as previously described [5]. Briefly, genomic DNA was extracted from the liver, and lambda EG10 DNA (48 kb) was rescued as the lambda phage by in vitro packaging. For 6-TG selection, the packaged phage was incubated with *E. coli* YG6020, which expresses Cre recombinase, and converted to a plasmid carrying *gpt* and chloramphenicol acetyltransferase. Infected cells were mixed with molten soft agar and poured onto agar plates containing chloramphenicol and 6-TG. In order to determine the total number of rescued plasmids, 3000-fold diluted phages were used to infect YG6020, and were poured on the plates containing chloramphenicol without 6-TG. The plates were incubated at 37°C for the selection of 6-TG-resistant colonies. Positively selected colonies were counted on d 3 and collected on d 4. The MF was calculated by dividing the number of *gpt* mutants after clonal correction by the number of rescued phages.

For the Spi$^-$ selection, the packaged phage was incubated with *E. coli* XL-1 Blue MRA for survival titration and *E. coli* XL-1 Blue MRA P2 for mutant selection. Infected cells were mixed with molten lambda-trypticase soft agar and poured onto lambda-trypticase agar plates. Next day, plaques (Spi$^-$ candidates) were punched out with sterilized glass pipettes and the agar plugs were suspended in SM buffer. In order to confirm the Spi$^-$ phenotype of candidates, the suspensions were spotted on three types of plates where XL-1 Blue MRA, XL-1 Blue MRA P2, or WL95 P2 strains were spread with soft agar. The real Spi$^-$ mutants, which made clear plaques on every plate, were collected and stored as phage lysates at 4°C. Approximate deletion sizes of the Spi$^-$ mutants were determined by agarose gel electrophoresis of the PCR-amplified target sequence.

For characterizing the mutation spectra of *gpt* mutants, a 739 bp DNA fragment containing the 456 bp coding region of the *gpt* gene was amplified by PCR as described previously [5]. DNA sequencing was performed with Big Dye™ Terminater Cycle Sequencing Ready Reaction (Applied Biosystems, Foster City, CA) on an ABI PRISM™ 310 Genetic Analyzer (Applied Biosystems).

Statistical Evaluation

For statistical analysis, the Student's *t*-test was used to compare liver and body weights, and quantitative data for GST-P positive liver cell foci and MFs between groups.

RESULTS

Growth of Animals, Liver Weights, and Chemical Intake

Data for final body and organ weights, and intake of test chemicals are shown in Table 1. The final body weight was not affected by any treatment during the experiment. Daily intakes of IQ, NPYR, and DEHP calculated from the consumption of diet or water were comparable to those in previous studies which showed significant carcinogenicity in rats [8,17,21]. Liver/body weight ratios were significantly ($P < 0.01$) increased in all rats that received chemicals, suggesting sufficient dosing. Especially, marked hepatomegaly was observed in the DEHP-treated rats ($P < 0.01$) with an increase to 183% of the nontreatment control value.

Histopathology and Immunohistochemical Analysis of GST-P

Histopathologically altered, mostly clear, hepatocellular foci were frequently observed in the IQ-treated and NPYR-treated rats (Figure 1A and C).

Table 1. Body and Liver Weights, and Food, Water, and Chemical Intake Data

Treatment	Number of rats	Body weight (g)[a]	Liver/body weight ratio (%)[a]	Food intake (g/rat/d)	Water intake (mL/rat/d)	Chemical intake	
						Total (mg/rat)	Daily (mg/rat/d)
IQ	5	264.6 ± 22.7	3.32 ± 0.11*	14.3	—	362	4.0
NPYR	5	257.8 ± 10.9	3.25 ± 0.16*	13.6	17.1	310	3.4
DEHP	5	279.3 ± 36.6	4.98 ± 0.28**	14.0	—	17 010	187.0
AAP	5	266.5 ± 11.4	3.40 ± 0.29*	15.6	—	12 740	140.0
Control	5	269.6 ± 27.0	2.72 ± 0.21	13.3	23.2	—	—

IQ, 2-amino-3-methylimidazo[4,5-*f*]quinoline; NPYR, *N*-nitrosopyrrolidine; DEHP, di(2-ethylhexyl)phthalate; AAP, acetaminophen.
[a]Data are mean ± SD values.
*$P < 0.01$ (vs. control).
**$P < 0.01$ (vs. IQ, NPYR, AAP, and control).

GST-P-positive liver cell foci (Figure 1B and D) corresponding to such altered foci were significantly ($P < 0.01$ and $P < 0.05$) increased in the IQ-treated and NPYR-treated groups in terms of number as well as area, but few were observed in the DEHP-treated, AAP-treated, and untreated control rats (Table 2). NPYR at a dose of 200 ppm was much more effective at inducing GST-P-positive foci than IQ at a dose of

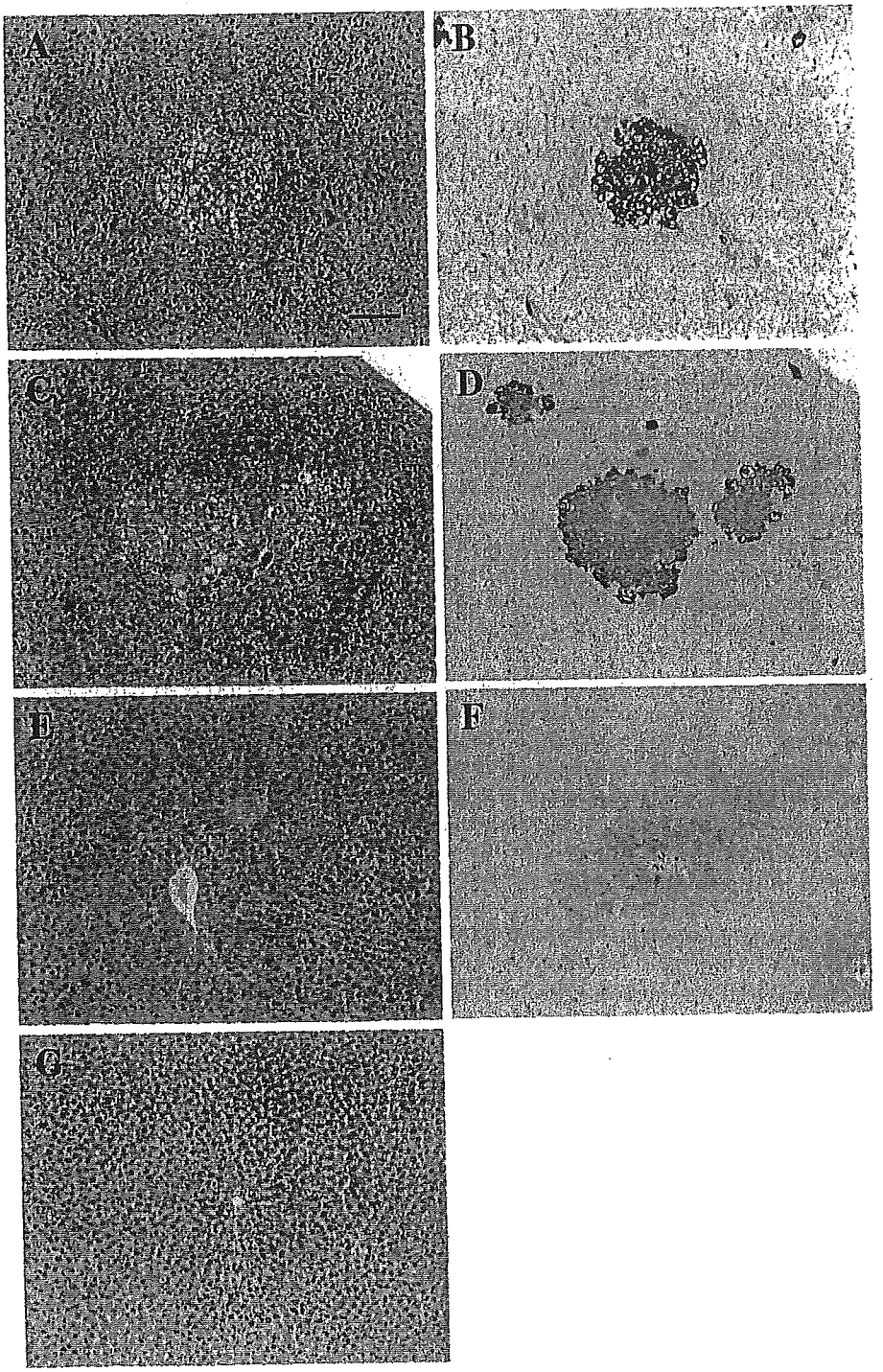

Figure 1. Histopathological findings (A, C, E, G) and immunohistochemistry for glutathione *S*-transferase placental form (GST-P) (B, D, F). Clear cell foci in the liver of rats given 2-amino-3-methylimidazo[4,5-*f*]quinoline (IQ) (A) and *N*-nitrosopyrrolidine (NPYR) (C). GST-P stainability corresponding to the foci A and C is evident (B and D). Marked centrilobular hypertrophy of liver cells is observed in a rat treated with di(2-ethylhexyl)phthalate (DEHP) (E). Faint and insignificant stainability of GST-P is found around the central veins of the liver of a rat treated with acetaminophen (AAP) (F). Appearance of the intact liver of a nontreated rat (G). Original magnification: ×180, Bar: 100 μm

Table 2. Numbers and Areas of GST-P Positive Liver Cell Foci

Treatment	Number of rats	Dose (ppm)	Number of foci/cm^2[a]	Area of foci (mm^2/cm^2)[a]
IQ	5	300	5.06 ± 1.52**	0.15 ± 0.06**
NPYR	5	200	24.05 ± 18.95*,***	1.09 ± 1.14*
DEHP	5	12 000	0.25 ± 0.17	<0.01
AAP	5	10 000	0.62 ± 0.44	<0.01
Control	5	—	0.48 ± 0.46	<0.01

[a]Data are mean ± SD values.
*$P < 0.05$ (vs. control).
**$P < 0.01$ (vs. control).
***$P < 0.05$ (vs. IQ).

300 ppm. Moreover, it was noteworthy that GST-P-positive single hepatocytes, which were not counted as the foci, were frequently observed in livers of the NPYR-treated rats. In the DEHP-treated rats, marked centrilobular hypertrophy of hepatocytes was observed throughout the whole liver (Figure 1E), although GST-P was consistently negative. In the AAP-treated rats, faint stainability for GST-P was detected in liver cells around the central veins, but these were not regarded as foci because of differences in staining intensity and diffuse location (Figure 1F).

Mutation Assays

Data for *gpt* MFs analyzed by 6-TG selection are summarized in Table 3. Identical mutations occurring in the same individual were omitted to avoid possible overlapping due to clonal proliferation. In the IQ-treated and NPYR-treated rats, *gpt* MFs in the liver DNA after clonal correction numbered 188.0×10^{-6} and 56.5×10^{-6}, approximately 35-fold and 10-fold higher, respectively, than the nontreatment control value (5.5×10^{-6}). There were no increases of *gpt* MFs in the liver DNA of the DEHP-treated (3.3×10^{-6}) and AAP-treated rats (5.5×10^{-6}) as compared to the nontreatment control value.

The *gpt* mutation spectra were analyzed by sequencing the *gpt* gene amplified from the mutants (Table 4). Because several mutants had two mutations in the *gpt* gene, the total number of mutations was larger than the number of mutants. In the IQ-treated rats, the predominant type of base substitution was the G:C to T:A transversion (62/109 = 56.9%), 45.2% (28/62) of which occurred at 5′-CpG-3′ sites. Most deletions occurred at G:C base pairs (9/10). In the NPYR-treated rats, the predominant type of base substitution was the A:T to G:C transition (33/67 = 49.3%) which was rare in the other groups. The numbers of G:C base substitutions were similar to the control levels. In the nontreatment control, DEHP-treated and AAP-treated rats, the most frequently observed mutation was the G:C to A:T transition. A:T to T:A transversions were observed in common in all the groups at a steady rate (18.2–34.8%). Most of them occurred at the same A:T base pair, the 299th in the *gpt* gene regardless of the experimental treatment.

Spi$^-$ selection for deletion mutations was performed for the DEHP-treated and nontreatment control cases. Spi$^-$ MFs were 4.5×10^{-6} and 4.3×10^{-6}, respectively (Table 5). Percentages of deletions larger than 1 kbp were 24.2 and 23.8 in the DEHP-treated and control rats, respectively. Thus, there were no differences in Spi$^-$ MF and deletion size spectrum between the DEHP-treated and control rats.

DISCUSSION

In order to understand the molecular mechanisms underlying chemical carcinogenesis in rats, *gpt* delta transgenic rats were here exposed to three established rodent hepatocarcinogens for 13-wk and

Table 3. Guanine Phosphoribosyltransferase (*gpt*) Mutant Frequencies (MFs) in the Liver

Treatment	Number of rats	Total population	Total *gpt* mutants	*gpt* mutants (clonal correction)	MF ($\times 10^{-6}$)[a]
IQ	5	525 000	133	89	188.0 ± 44.9*
NPYR	5	1 021 500	57	49	56.5 ± 24.5*,**
DEHP	5	3 247 500	9	9	3.3 ± 3.8
AAP	5	3 637 500	19	17	5.5 ± 5.6
Control	5	2 976 000	19	16	5.5 ± 2.4

[a]Data are mean ± SD values.
*$P < 0.01$ (vs. control).
**$P < 0.01$ (vs. IQ).

Table 4. Mutation Spectra of *gpt* Mutant Colonies

Type	Treatment				
	IQ	NPYR	DEHP	AAP	Control
Base substitution					
Transition					
G:C to A:T	6 (5.5)	5 (7.5)	5 (45.5)	9 (39.1)	8 (38.1)
A:T to G:C	1 (0.9)	33 (49.3)	0 (0)	0 (0)	0 (0)
Transversion					
G:C to T:A	62 (56.9)	3 (4.5)	3 (27.3)	5 (21.7)	2 (9.5)
G:C to C:G	1 (0.9)	0 (0)	0 (0)	0 (0)	0 (0)
A:T to T:A	26 (23.9)	20 (29.9)	2 (18.2)	8 (34.8)	7 (33.3)
A:T to C:G	1 (0.9)	3 (4.5)	0 (0)	0 (0)	0 (0)
Deletion	10 (9.2)	2 (3.0)	1 (9.1)	1 (4.3)	4 (19.0)
−1 bp	9	0	1	1	4
>2 bp	1	2	0	0	0
Insertion	0 (0)	0 (0)	0 (0)	0 (0)	0 (0)
Others	2 (1.8)	1 (1.5)	0 (0)	0 (0)	0 (0)
Total number of mutation	109 (100)	67 (100)	11 (100)	23 (100)	21 (100)

Numbers in parentheses are percentages.

in vivo mutation assays were performed. GST-P positive liver cell foci were significantly induced by IQ and NPYR, and marked hepatomegaly characterized by centrilobular hypertrophy of hepatocytes was observed in the DEHP-treated rats. Because these alterations are known as early intermediate endpoint lesions for rat hepatocarcinogenesis [32,33], the findings strongly suggest that the doses of these chemicals were sufficient to elicit carcinogenic responses in the livers of *gpt* delta rats in the present study. NPYR at a dose of 200 ppm induced more GST-P lesions than IQ at a dose of 300 ppm, indicating that NPYR is more carcinogenic in the present study, which is compatible with the previous carcinogenicity bioassays reporting 14/15 (93%) and 18/40 (45%) of tumor incidences with NPYR and IQ under the same condition, respectively [8,17]. However, MFs in the *gpt* target gene determined by 6-TG selection were three-times higher in the IQ-treated rats than in the NPYR-treated rats, indicating that the MF itself is not directly correlated with the carcinogenic activity of each compound. In the present mutagenicity assay, the MFs were determined from the mutation occurring in the reporter gene, which has no biological function. Carcinogenesis, however, should require the crucial mutations in the cancer-related genes for the initiation, and also promotional factors for the tumor development. Thus, it is not inconsistent that the carcinogenicity does not necessarily correlate with the in vivo mutagenicity simply in terms of intensity.

In vivo mutagenicity and mutation spectrum of IQ have been investigated in commercially available transgenic rodent models such as MutaMouse and BigBlue [20,34,35]. Because IQ is widely known to be a potent mutagen for the liver and induces mainly G:C to T:A transversion, it was used as an appropriate positive mutagen for validating the mutagenicity assay system. As expected, IQ proved positive, causing G:C to T:A transversions and deletions at G:C base pairs, confirming the reliability of *gpt* delta rats for in vivo mutagenicity assays. In view of the molecular mechanisms, two types of direct DNA adducts, the major *N*-(deoxyguanosin-8-yl)-IQ and the minor 5-(deoxyguanosin-N^2-yl)-IQ, are thought to be responsible for IQ-mutagenesis [19,36]. It has also been suggested that oxidative DNA damage with 8-OHdG formation as a result of nonenzymatic reduction of nitro-IQ may play a role in carcinogenesis [37]. Although, we could not determine which

Table 5. Spi$^-$ MFs in the Liver

Treatment	Number of rats	Total population	Total Spi$^-$ mutants	MF ($\times 10^{-6}$)[a]	Deletion size	
					<1 kb (%)	>1 kb (%)
DEHP	5	7 354 500	33	4.5 ± 2.5	25 (75.8)	8 (24.2)
Control	5	9 340 500	42	4.3 ± 2.5	32 (76.2)	10 (23.8)

[a]Data are mean ± SD values.

type of DNA lesion was responsible for the IQ-induced hepatocarcinogenesis, recent work with a panel of biomarkers for detecting oxidative stress, DNA damage, and expression of DNA repair enzymes in IQ-treated BigBlue rats pointed to specific DNA adducts rather than oxidative DNA damage as responsible for IQ initiation of hepatocarcinogenesis [38].

DEHP is categorized as a nongenotoxic carcinogen because it induces liver tumors in both sexes of rats and mice in a dose-dependent manner [21], with *Salmonella* in vitro mutagenicity assay being uniformly negative [22,23]. To the best of our knowledge, however, there is only one report testing in vivo mutagenicity of several nongenotoxic carcinogens, including DEHP, in *lacI* transgenic mice, which failed to detect mutagenicity [39]. In the present study, point mutations and deletion mutations were widely screened by 6-TG selection and Spi$^-$ selection, respectively, in order to analyze the possible involvement of genotoxicity caused by reactive metabolites or peroxisomal oxidative stress. However, no mutagenic activity of DEHP was detected in the liver of *gpt* delta rats after 13-wk of treatment. In the DEHP-treated rats, 27.3% of the total mutations were G:C to T:A transversions, known to be caused by 8-OHdG [40], while this was the case for 9.5% in the control rats. Because the *gpt* delta rat has relatively few copies of the transgene lambda EG10, the total number of mutants obtained was too small to allow accurate evaluation of the specific mutation spectrum, but the results do suggest that hepatocarcinogenesis by DEHP in rodents mainly depends on nongenotoxic or promotional mechanisms rather than direct DNA damage.

Despite extensive studies on the metabolism of NPYR or DNA modification by its metabolites, the in vivo mutation spectrum of NPYR in the mammalian species has not yet been determined. In the present study, NPYR predominantly induced A:T to G:C transitions in the liver of the *gpt* delta rats, accounting for 49.3% of all mutations in the *gpt* gene. This was unexpected because there have been a sufficient number of studies for providing specific adduct formations by NPYR with deoxyguanosine. NPYR is metabolically activated via alpha-hydroxylation by cytochrome P450 enzymes to yield reactive intermediates, 4-hydroxybutylaldehyde, and crotonaldehyde [41]. These metabolites can alkylate deoxyguanosine, and mainly result in exocyclic adducts such as N^7,C-8 guanine adducts and 1,N^2-propanodeoxyguanosine [42]. Because these adducts have also been found in DNA from tissues of NPYR- or crotonaldehyde-treated animals, they might be expected to be the major adducts formed in vivo [43,44]. NPYR-induced mutational spectra have been investigated in bacterial systems with the *lacI* gene and M13mp2 phage DNA as targets [12,13] and base substitutions at G:C base pairs appeared to predominate. In the present study, however, the predominant type of base substitution in the liver of NPYR-treated rats was evidently A:T to G:C, followed by A:T to T:A. The difference between in vitro and in vivo mutagenesis by NPYR may be partly explained by means of specific etheno-adduct formation due to reactions of crotonaldehyde with deoxyadenosine as well as deoxyguanosine, known to yield 1,N^6-ethenoadenosine [45]. This latter adduct is formed during lipid peroxidation [46], and has also been detected in tissues from rats treated with vinyl chloride, a hepatocarcinogen in humans and rodents [47]. In the present study, the livers of NPYR-treated rats contained a number of GST-P positive single liver cells which may be indicative of lipid peroxidation and its end products, unsaturated aldehydes such as 4-hydroxynonenal, acrolein, and crotonaldehyde [48]. 1,N^6-Ethenoadenosine has shown to be highly mutagenic in mammalian cells such as simian kidney cells, exclusively inducing A:T to G:C base substitutions, while the mutation efficiency in *E. coli* is relatively low [49]. Moreover, Barbin et al. have suggested that concomitant formation of the etheno-adducts may play a role in the hepatocarcinogenesis by vinyl chloride, due to A:T base mutation occurring in the *p53* tumor suppressor gene [50]. In addition to a possible metabolite, crotonaldehyde, from NPYR, these data thus provide a possible mutational mechanism mediated by lipid peroxidation, interpreting our present findings in NPYR-treated rats. For understanding the molecular mechanism of NPYR-induced hepatocarcinogenesis, the levels of mutagenic adenine or thymine adducts and the possible specific mutations in the cancer-related genes need to be further analyzed in the liver of NPYR-treated rats.

In conclusion, based on the characteristic mutation spectra here observed in IQ-treated and NPYR-treated *gpt* delta transgenic rats, the predominant occurrence of A:T to G:C transitions in the NPYR-case suggests a possible contribution of the minor adenine adduct 1,N^6-ethenoadenosine to its in vivo mutagenesis in mammals, even though this carcinogen has been reported to form mainly guanine adducts in vitro. No mutagenic activity was detected in DEHP-treated rats, supporting the promotion pathway of DEHP-induced hepatocarcinogenesis rather than direct DNA damage. Our data also indicate that analysis of the specific in vivo mutational spectrum can provide crucial information for understanding the molecular mechanisms underlying chemical carcinogenesis.

ACKNOWLEDGMENTS

We thank all individuals of Division of Genetics and Mutagenesis, National Institute of Health Sciences for technical advices and valuable suggestions for the mutation assays. This work was supported in part by a grant for Research Fellow of the Japan Society for the Promotion of Science, a

Grant-in-aid (12-9) for Cancer Research from the Ministry of Health, Labor, and Welfare of Japan, and a Grant-in-aid (13670235) for Scientific Research from the Ministry of Education, Culture, Sports, Science, and Technology of Japan.

REFERENCES

1. Lijinsky W. Carcinogenicity and mutagenicity of *N*-nitroso compounds. Mol Toxicol 1987;1:107–119.
2. Tennant RW, Elwell MR, Spalding JW, Griesemer RA. Evidence that toxic injury is not always associated with induction of chemical carcinogenesis. Mol Carcinog 1991;4: 420–440.
3. Crebelli R, Conti L, Fuselli S, Leopardi P, Zijno A, Carere A. Further studies on the comutagenic activity of cigarette smoke condensate. Mutat Res 1991;259:29–36.
4. Godard T, Fessard V, Huet S, et al. Comparative in vitro and in vivo assessment of genotoxic effects of etoposide and chlorothalonil by the comet assay. Mutat Res 1999;444: 103–116.
5. Nohmi T, Suzuki T, Masumura K. Recent advances in the protocols of transgenic mouse mutation assays. Mutat Res 2000;455:191–215.
6. Hayashi H, Kondo H, Masumura K, Shindo Y, Nohmi T. Novel transgenic rat for in vivo genotoxicity assays using 6-thioguanine and Spi^- selection. Environ Mol Mutagen 2003;41:253–259.
7. Nohmi T, Katoh M, Suzuki H, et al. A new transgenic mouse mutagenesis test system using Spi^- and 6-thioguanine selections. Environ Mol Mutagen 1996;28:465–470.
8. Lijinsky W, Taylor HW. The effect of substituents on the carcinogenicity of *N*-nitrosopyrrolidine in Sprague-Dawley Rats. Cancer Res 1976;36:1988–1990.
9. Bartsch H, O'Neill IK, Castegnaro M, Okada M. Evaluation of the carcinogenic risk of chemicals to humans: Some *N*-nitroso compounds. IARC Sci Publ 1978;39:313–326.
10. Wang M, MacIntee EJ, Shi Y, et al. Reactions of alpha-acetoxy-*N*-nitrosopyrrolidine with deoxyguanosine and DNA. Chem Res Toxicol 2001;14:1435–1445.
11. Guttenplan JB. *N*-nitrosamines: Bacterial mutagenesis and in vitro metabolism. Mutat Res 1987;186:81–134.
12. Ziellenska M, Ahmed A, Glickman BW. Mutational specificities of environmental carcinogens in the *lacI* gene of *Escherichia coli*. III: The cyclic nitrosamine *N*-nitrosopyrrolidine is a complex mutagen. Mol Carcinog 1990;3:122–125.
13. Arimoto KS, Anma N, Yoshinaga Y, Douki T, Cadet J, Hayatsu H. Oxidative damage and induced mutations in m13mp2 phage DNA exposed to *N*-nitrosopyrrolidine with UVA radiation. Mutagenesis 2000;15:473–477.
14. IARC. IQ (2-amino-3-methylimidazo[4,5-*f*]quinoline). In: Some naturally occurring substances: Food items and constituents, heterocyclic aromatic amines and mycotoxins. IARC monograph on the evaluation of carcinogenic risk of chemicals to humans. 1993;56:165–195.
15. Griciute L. Carcinogenicity of *N*-nitroso compounds and their possible role in the development of human cancer. IARC Sci Publ 1978;18:3–9.
16. Yamashita M, Wakabayashi K, Nagao M, et al. Detection of 2-amino-3-methylimidazo[4,5-*f*]quinoline in cigarette smoke condensate. Jpn J Cancer Res (Gann) 1986;77:419–422.
17. Ohgaki H, Hasegawa H, Kato T, et al. Carcinogenicity in mice and rats of heterocyclic amines in cooked foods. Environ Health Perspect 1986;67:129–134.
18. Adamson RH, Thorgeirsson UP, Snyderwine EG, et al. Carcinogenicity of 2-amino-3-methylimidazo[4,5-*f*]quinoline in non-human primates: Induction of tumors in three macaques. Jpn J Cancer Res 1990;81:10–14.
19. Schut HAJ, Snyderwine EG. DNA adducts of heterocyclic amine food mutagens: Implications for mutagenesis and carcinogenesis. Carcinogenesis 1999;20:353–368.
20. Bol SA, Horlbeck J, Markovic J, de Boer JG, Turesky RJ, Constable A. Mutational analysis of the liver, colon, and kidney of BigBlue rats treated with 2-amino-3-methylimidazo[4,5-*f*]quinoline. Carcinogenesis 2000;21:1–6.
21. Kluwe WM, McConnell EE, Huff JE, Haseman JK, Douglas JF, Hartwell WV. Carcinogenicity testing of phthalate esters and related compounds by the National Toxicology Program and the National Cancer Institute. Environ Health Perspect 1982; 45:129–133.
22. Kirby PE, Pizzarello RF, Lawlor TE, Haworth SR, Hodgson JR. Evaluation of di-(2-ethylhexyl)phthalate and its major metabolites in the Ames test and L5178Y mouse lymphoma mutagenicity assay. Environ Mutagen 1983;5: 657–663.
23. Zeiger E, Haworth S, Mortelmans K, Speck W. Mutagenicity testing of di(2-ethylhexyl)phthalate and related chemicals in *Salmonella*. Environ Mutagen 1985;7:213–232.
24. Yagi YK, Shimoi N. Teratogenicity and mutagenicity of a phthalate ester. Teratology 1976;14:259–260.
25. Tomita I, Nakamura Y, Aoki N, Inui N. Mutagenic/carcinogenic potential of DEHP and MEHP. Environ Health Perspect 1982;45:119–125.
26. Takagi A, Sai K, Umemura T, Hasegawa R, Kurokawa Y. Significant increase of 8-hydroxydeoxyguanosine in liver DNA of rats following short-term exposure to the peroxisome proliferators di-(2-ethylhexyl)phthalate and di-(2-ethylhexyl)adipate. Jpn J Cancer Res 1990;81:213–215.
27. Seo KW, Kim KB, Kim YJ, Choi JY, Lee KT, Choi KS. Comparison of oxidative stress and changes of xonobiotic metabolizing enzymes induced by phthalates in rats. Food Chem Toxicol 2004;42:107–114.
28. Gorelick NJ. Overview of mutation assays in transgenic mice for routine testing. Environ Mol Mutagen 1995;25: 218–230.
29. Mirsalis JC, Monforte JA, Wineger RA. Transgenic animal models for detection of in vivo mutations. Ann Rev Pharmacol Toxicol 1995;35:145–164.
30. de Boer JG. Protection by dietary compounds against mutation in a transgenic rodent. J Nutr 2001;131:3082S–3086S.
31. Nishikawa A, Suzuki T, Masumura K, et al. Reporter gene transgenic mice as a tool for analyzing the molecular mechanisms underlying experimental carcinogenesis. J Exp Clin Cancer Res 2001;20:111–115.
32. Ito N, Hasegawa R, Imaida K, et al. Medium-term rat liver bioassay for rapid detection of hepatocarcinogenic substances. J Toxicol Pathol 1997;10:1–11.
33. Takagi A, Sai K, Umemura T, Hasegawa R, Kurokawa Y. Hepatomegaly is an early biomarker for hepatocarcinogenesis induced by peroxisome proliferators. J Environ Pathol Toxicol Oncol 1992;11:145–149.
34. Ushijima T, Hosoya Y, Ochiai M, et al. Tissue-specific mutational spectra of 2-amino-3,4-dimethylimidazo[4,5-*f*]quinoline in the liver and bone marrow of *lacI* transgenic mice. Carcinogenesis 1994;15:2805–2809.
35. Davis CD, Dacquel HAJ, Schut SS, Thorgeirsson SS, Snyderwine EG. In vivo mutagenicity and DNA adduct levels of heterocyclic amines in Muta™Mice and c-*myc*/*lacZ* double transgenic mice. Mutat Res 1996;356:287–296.
36. Turesky RJ, Gremaud E, Markovic J, Snyderwine EG. DNA adduct formation of the food-derived mutagen 2-amino-3,4-dimethylimidazo[4,5-*f*]quinoline in nonhuman primates undergoing carcinogen bioassay. Chem Res Toxicol 1996;9: 403–408.
37. Murata M, Kobayashi M, Kawanishi S. Nonenzymatic reduction of nitro derivative of a heterocyclic amine IQ by NADH and Cu(II) leads to oxidative DNA damage. Biochemistry 1999;38:7624–7629.

38. Moller P, Wallin H, Vogel U, et al. Mutagenicity of 2-amino-3-methylimidazo[4,5-*f*]quinoline in colon and liver of BigBlue rats: Role of DNA adducts, strand breaks, DNA repair, and oxidative stress. Carcinogenesis 2002;23:1379–1385.
39. Gunz D, Shephard SE, Lutz WK. Can nongenotoxic carcinogens be detected with the *lacI* transgenic mouse mutation assay? Environ Mol Mutagen 1993;21:209–211.
40. Moriya M. Single-stranded shuttle phagemid for mutagenesis studies in mammalian cells: 8-oxoguanine in DNA induces targeted G:C-T:A transversions in simian kidney cells. Proc Natl Acad Sci USA 1993;90:1122–1126.
41. Wang M, Chung FL, Hecht SS. Identification of crotonaldehyde as a hepatic microsomal metabolite formed by alpha-hydroxylation of the carcinogen *N*-nitrosopyrrolidine. Chem Res Toxicol 1988;1:28–31.
42. Wang M, Chung FL, Hecht SS. Formation of acyclic and cyclic guanine adducts in DNA reacted with α-acetoxy-*N*-nitrosopyrrolidine. Chem Res Toxicol 1989;2:423–428.
43. Hunt EJ, Shank RC. Formation and persistence of a DNA adduct in rodents treated with *N*-nitrosopyrrolidine. Carcinogenesis 1991;12:571–575.
44. Chung FL, Young R, Hecht SS. Detection of cyclic 1,N^2-propanodeoxyguanosine adducts in DNA of rats treated with *N*-nitrosopyrrolidine and mice treated with crotonaldehyde. Carcinogenesis 1989;10:1291–1297.
45. Chen HJ, Chung FL. Formation of etheno adducts in reactions of enals via autoxidation. Chem Res Toxicol 1994;7:857–860.
46. el Ghissassi F, Barbin A, Nair J, Bartsch H. Formation of 1,N^6-ethenoadenine and 3,N^4-ethenocytosine by lipid peroxidation products and nucleic acid bases. Chem Res Toxicol 1995;8:278–283.
47. Guichard Y, el Ghissassi F, Nair J, Bartsch H, Barbin A. Formation and accumulation of DNA ethenobases in adult Sprague-Dawley rats exposed to vinyl chloride. Carcinogenesis 1996;17:1553–1559.
48. Satoh K, Hayakari M, Ookawa K, et al. Lipid peroxidation end products-responded induction of a preneoplastic marker enzyme glutathione *S*-transferase P-form (GST-P) in rat liver on administration via the portal vein. Mutat Res 2001;483:65–72.
49. Pandya GA, Moriya M. 1,N^6-ethenodeoxyadenosine, a DNA adduct highly mutagenic in mammalian cells. Biochemistry 1996;35:11487–11492.
50. Barbin A, Froment O, Boibin S, et al. *p53* Gene mutation pattern in rat liver tumor induced by vinyl chloride. Cancer Res 1997;57:1695–1698.

Available online at www.sciencedirect.com
SCIENCE DIRECT®
DNA Repair 4 (2005) 1160–1171
DNA REPAIR
www.elsevier.com/locate/dnarepair

Roles of replicative and specialized DNA polymerases in frameshift mutagenesis: Mutability of *Salmonella typhimurium* strains lacking one or all of SOS-inducible DNA polymerases to 26 chemicals

Kiyoko Kokubo [a,b], Masami Yamada [a], Yusuke Kanke [b], Takehiko Nohmi [a,*]

[a] *Division of Genetics and Mutagenesis, National Institute of Health Sciences, 1-18-1, Kamiyoga, Setagaya-ku, Tokyo 158-8501, Japan*
[b] *Graduate School of Home Economics, Otsuma Women's University, 12 Sanban-cho, Chiyoda-ku, Tokyo 102-8357, Japan*

Received 26 March 2005; received in revised form 7 June 2005; accepted 9 June 2005
Available online 15 August 2005

Available online at www.sciencedirect.com
SCIENCE DIRECT
DNA Repair 4 (2005) 1160–1171
DNA REPAIR
www.elsevier.com/locate/dnarepair

Roles of replicative and specialized DNA polymerases in frameshift mutagenesis: Mutability of *Salmonella typhimurium* strains lacking one or all of SOS-inducible DNA polymerases to 26 chemicals

Kiyoko Kokubo [a,b], Masami Yamada [a], Yusuke Kanke [b], Takehiko Nohmi [a,*]

[a] *Division of Genetics and Mutagenesis, National Institute of Health Sciences, 1-18-1, Kamiyoga, Setagaya-ku, Tokyo 158-8501, Japan*
[b] *Graduate School of Home Economics, Otsuma Women's University, 12 Sanban-cho, Chiyoda-ku, Tokyo 102-8357, Japan*

Received 26 March 2005; received in revised form 7 June 2005; accepted 9 June 2005
Available online 15 August 2005

Abstract

Progression of DNA replication is occasionally blocked by endogenous and exogenous DNA damage. To circumvent the stalling of DNA replication, cells possess a variety of specialized DNA polymerases that replicate through DNA damage. *Salmonella typhimurium* strain TA1538 has six DNA polymerases and four of them are encoded by damage-inducible SOS genes, i.e. $polB_{ST}$ (pol II), $dinB_{ST}$ (pol IV), $umuDC_{ST}$ (pol V) and *samAB*. The strain has been used for the detection of a variety of chemical mutagens because of the high sensitivity to −2 frameshift occurring in CGCGCGCG sequence. To assign the role of each DNA polymerase in the frameshift mutagenesis, we have constructed the derivatives lacking one or all of SOS-inducible DNA polymerases and examined the mutability to 26 chemical mutagens. Interestingly, the chemicals could be categorized into four classes: class I whose mutagenicity was reduced by the deletion of $dinB_{ST}$ (1-aminoanthracene and other four chemicals); class II whose mutagenicity was reduced by the deletion of either $dinB_{ST}$ or $umuDC_{ST}$ plus *samAB* (7,12-dimethylbenz[*a*]anthracene and other three chemicals); class III whose mutagenicity largely depended on the presence of $umuDC_{ST}$ plus *samAB* (1-*N*-6-azabenzo[*a*]pyrene and other three chemicals) and class IV whose mutagenicity was not reduced by deletion of any of the genes encoding SOS-inducible DNA polymerases (Glu-P-1 and other 12 chemicals). Deletion of $polB_{ST}$ reduced by 30–60% the mutagenicity of six chemicals of classes II and III. These results suggest that multiple DNA polymerases including the replicative DNA polymerase, i.e. DNA polymerase III holoenzyme, play important roles in chemically induced −2 frameshift and also that different sets of DNA polymerases are engaged in the translesion bypass of different DNA lesions.

Keywords: SOS-inducible DNA polymerases; Translesion DNA synthesis; Frameshift; Mutagens; Replicative DNA polymerase

1. Introduction

Cellular DNA is continuously exposed to a variety of endogenous and exogenous mutagens. Ultraviolet light radiation and exposure to chemical carcinogens induce DNA adducts and reactive oxygen species oxidize bases in DNA. Although most of these lesions are removed by nucleotide excision repair and base excision repair, the repair mechanisms are not fully efficient and some lesions persist in the DNA [1]. The attempt to replicate damaged template DNA usually leads to stalling of replicative DNA polymerase and thus formation of single-stranded DNA gap region downstream of the lesion. To fill in the gap, two major pathways are in operation. One is a recombination mechanism, which consists of filling in the gap with a homologous DNA sequence that is derived from the replicated sister chromatids [2]. The other pathway is translesion DNA synthesis (TLS), which directly bypasses the lesion and fills in the gap [3–6]. In fact, cells are endowed with multiple DNA polymerases to bypass a variety of DNA damage [7]. Some TLS reactions are error-prone, i.e. incorporating incorrect bases in the nascent strand, while others are error-free [8]. Thus, TLS appears to contribute to mutagenesis and DNA damage tolerance.

* Corresponding author. Tel.: +81 3700 9873; fax: +81 3 3707 6950.
E-mail address: nohmi@nihs.go.jp (T. Nohmi).

1568-7864/$ – see front matter © 2005 Elsevier B.V. All rights reserved.
doi:10.1016/j.dnarep.2005.06.016